2016

Theoretical and Experimental Analysis of Expansion Devices for Meso-Scale Cooling Systems

João Fabio Parise de Lara
Federal University of Santa Catarina, Brazil, joao@polo.ufsc.br

Claudio Melo
Federal University of Santa Catarina, Brazil, melo@polo.ufsc.br

Joel Boeng
Federal University of Santa Catarina, Brazil, joel@polo.ufsc.br

Theoretical and Experimental Analysis of Expansion Devices for Meso-Scale Cooling Systems

João F. P. DE LARA, Cláudio MELO*, Joel BOENG

POLO – Research Laboratories for Emerging Technologies in Cooling and Thermophysics
Department of Mechanical Engineering, Federal University of Santa Catarina
88040-900, Florianópolis, SC, Brazil, +55 48 3721 7900

* Corresponding Author: melo@polo.ufsc.br

ABSTRACT

The aim of this research was to study the expansion process of HFC-134a through two distinct expansion devices applied in compact cooling systems, the so-called meso-scale cooling systems. To this end, an experimental apparatus was designed and built to mimic the running conditions of such systems. The experiments were planned according to the factorial design technique. The first part of this work was focused on small diameter adiabatic capillary tubes and showed that the capillary tube I.D. plays a major role in determining the refrigerant mass flow rate. It was also found that the models developed predicted 90% of the experimental data points within a band of error of ±10%. Visualization studies were also carried out and it was found that vapor bubbles at the entrance of the capillary tubes have a critical effect in meso-scale cooling systems. The second part of this work was focused on pulsating capillary tubes (series association of a PWM-driven metering valve, an intermediate chamber and an adiabatic capillary tube) and showed that the refrigerant mass flow rate is determined by the valve duty cycle. Unfortunately, the fluid flow phenomenon for this particular expansion device was not well captured by the model, with deviations of the order of ±30%.

1. INTRODUCTION

Although listed as a prioritized research area by the International Institute of Refrigeration (IIR, 2010), very few studies focused on meso-scale cooling systems are available in the literature. However, many examples of such systems are found in the electronics, personal and medical cooling areas. The power electronics field is the main driver of this new generation of cooling systems. Due to the increasing speed and decreasing size of the actual micro-chips, the heat release fluxes from these processors are growing steadily. Thus, high-capacity, small-sized cooling systems are needed. The miniaturization of mechanical systems, especially those of a thermal nature, is not an easy task. Jeong (2004), for example, conducted an entropy generation analysis and concluded that the smaller the cooling system the lower the coefficient of performance will be. In this context, expansion devices for meso-scale cooling systems need to be studied not only for performance improvement but also to guarantee the system integrity under different operating conditions.

Capillary tubes are widely used as expansion devices, mainly because of their simplicity and low cost. The great impact of this component on the system performance has stimulated a vast amount of applied and fundamental research work focused on the rather complex capillary tube flow (Bolstad and Jordan, 1948; Mikol and Dudley, 1964; Melo et al., 1999). However, meso-scale cooling systems usually require a relatively low mass flow rate, thereby requiring a considerably restricted expansion device. Regular I.D. capillary tubes are not suitable for such systems, unless they are extremely long. Thus, despite the advantages of using capillary tubes, their use in meso-scale cooling systems is somewhat challenging mainly because of the small diameters involved.

Variable opening expansion devices, on the other hand, offer the possibility of controlling the refrigerant mass flow rate according to the imposed thermal load, thus improving the system performance (Marcinichen et al., 2006, Zhang et al., 2006, Pottker, 2007 and Ronzoni et al., 2011). However, electronic expansion valves for meso-scale applications are not easily encountered in the market, especially because of the small orifice I.D. involved. A smarter option would be the use of a series association of a PWM (Pulse Width Modulation) valve with a capillary tube (Thiessen and Klein, 2007).

The aim of this research was to study the expansion process of HFC-134a through fixed and variable restriction expansion devices, focusing on meso-scale cooling systems. To this end, experiments were carried out on two fronts: (i) adiabatic capillary tube flow and ii) pulsating capillary tube flow. The mathematical models of Hermes (2006, 2010) for predicting the refrigerant mass flow rate in regular-scale refrigerating systems were tuned to the experimental data gathered. Finally, visualization studies were carried out for a better understanding of the inlet quality on the refrigerant mass flow rate provided by both expansion devices.

2. EXPERIMENTAL APPARATUS

An experimental apparatus was designed and built to mimic a meso-scale cooling system, working under typical operating conditions. The testing apparatus is basically comprised of two sub-systems: (i) a cooling loop and (ii) a test section. The cooling loop establishes and maintains the operating conditions while the test section can be either a stretched and thermal insulated capillary tube or a pulsating capillary tube. Both sub-systems are illustrated in Figure 1.

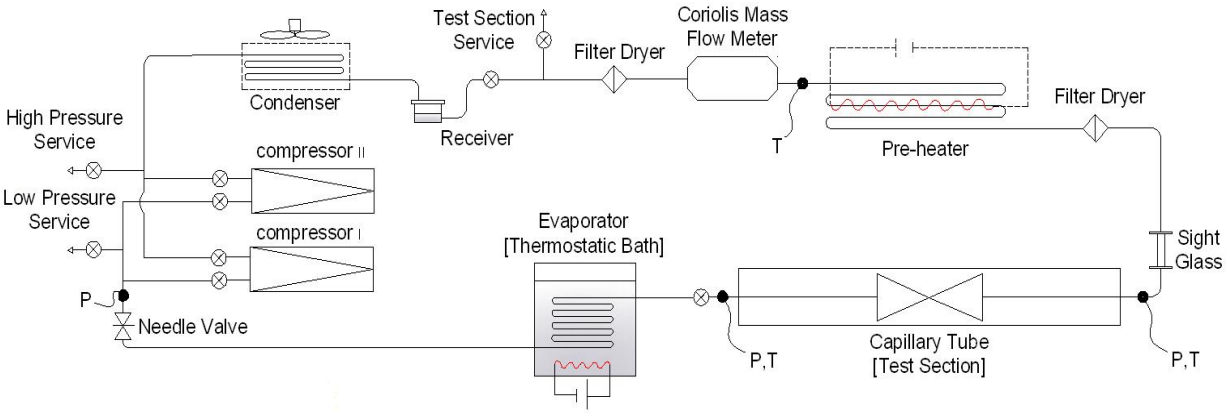

Figure 1: Schematic diagram of the testing apparatus

The cooling loop is comprised of a sight glass, an evaporator, a thermostatic bath, a needle valve, two linear oil-free compressors, a forced draft condenser, an accumulator, a Coriolis mass flow meter and an electrical pre-heater. The test section is essentially a copper capillary tube thermally insulated with two 15 mm-thick layers of high-density polyurethane foam. The condensing pressure is controlled by two PIV- driven variable speed axial fans. The liquid accumulator ensures that only liquid refrigerant reaches the mass flow meter. The pre-heater controls either the subcooling or the refrigerant quality at the entrance of the expansion device. The evaporation temperature is controlled by a thermostatic bath. A needle valve is installed at the compressor suction point to control the circulating mass flow rate. In some experiments a PWM valve and an intermediate chamber are installed upstream of the capillary tube.

3. TEST PLAN

The experiments were designed according to the Factorial Design Technique, in an attempt to reduce the number of data runs without losing the quality of the experiments. In this technique, factors and levels are chosen and the experiment is planned based on different combinations of them. Factorial design allows the evaluation of the effect of each independent variable, as well as the effect of the interactions among them on the dependent variable (Box et al., 1978).

3.1 Adiabatic capillary tubes

The first part of the experiments was focused on the refrigerant flow through adiabatic capillary tubes. Table 1 shows the chosen factors and levels, where the symbols (-), (+/-) and (+) represent the lower, intermediate and higher levels, respectively.

Table 1: Factors and levels for adiabatic capillary tubes

Factors	-	+/-	+
Capillary tube I.D. [mm]	0.23	0.39	0.45
Capillary tube length [m]	1	-	2
Condensing pressure [bar]	9	-	19
Subcooling [°C]	5	-	10

The diameter and length of the capillary tube, the condensing pressure and the subcooling were chosen as the independent factors, and the mass flow rate as the response-dependent factor (Gonçalves, 1994; Melo, 1999). Three levels were chosen for the inner diameter due to its non-linearity with the mass flow rate (Gonçalves, 1994). The combination of factors and levels provided an experimental database of 24 data points. Additionally, 20 experiments were carried out with 0.26mm, 0.38mm and 0.53mm I.D. capillary tubes, covering the range between meso- and regular-sized capillary tubes.

3.2 Pulsating capillary tubes

The second part of the experiments focused on pulsating capillary tubes (series association of a PWM valve, intermediate chamber and capillary tube). Table 2 shows the levels chosen for each independent factor. It is worth noting that the effect of the valve duty cycle was examined with three levels, as recommended by Ronzoni et al. (2011). The combination of factors and levels provided an experimental database of 96 data points. Additionally, 12 experiments were carried out with an intermediate flow coefficient valve.

Table 2: Factors and levels for pulsating capillary tubes

Factors	-	+/-	+
Duty cycle [%]	10	50	90
Pulse period [s]	1	-	4
Condensing pressure [bar]	9	-	16
Capillary tube I.D. [mm]	0.45	-	0.51
Flow coefficient [-]	2.7E-8	-	7.1E-8
Intermediate chamber internal volume [ml]	1	-	2

4. MATHEMATICAL ANALYSIS

In this section, mathematical models to predict the refrigerant flow through expansion devices of meso-scale cooling systems are briefly described. The first model is comprised of a set of differential equations and is capable of predicting not only the mass flow rate but also the refrigerant states along the capillary tube for any kind of working fluid (Hermes, 2006). In contrast, the second model relies on an algebraic and explicit equation for predicting the mass flow rate of HFC-134a or HC-600a through adiabatic capillary tubes. The model proposed by Ronzoni et al. (2011) is comprised of three sub-models and is capable of predicting the mass flow rate through pulsating capillary tubes.

4.1 Differential capillary tube model

In contrast to the approach of Hermes (2006), the friction factor and the refrigerant viscosity were estimated through the equations proposed by Churchill (1977) and Bittle and Weis (2002), respectively. The set of differential equations were integrated in the pressure domain through a second-order Runge Kutta method, as proposed by Hermes (2006). The equations were solved through a first-order Euler method (Carnahan et al., 1969). The refrigerant mass flow rate was interactively calculated because it is dependent on the capillary exit pressure. The mass flow rate values were updated based on the difference between the actual and estimated length of the capillary tube, as proposed by Melo et al. (1992).

4.2 Algebraic capillary tube model

The main disadvantage of differential models is the excessive computational time. Algebraic models, although to some extent limited, require a lower CPU time and are free of convergence issues. Several analytical models are

available in the literature, most of them requiring a certain level of computational complexity. This study adopted the semi-empirical model proposed by Hermes (2010), since it was derived from one of the most extensive and reliable experimental databases.

4.3 Pulsating capillary tube model

The model proposed by Ronzoni et al. (2011) is divided into three sub-models: valve, capillary tube and intermediate chamber. The capillary tube model is essentially the algebraic model introduced previously. The capillary tube and valve refrigerant mass flow rates are estimated explicitly, with the liquid level in the intermediate chamber resulting from the coupling between them. The chamber acts as a reservoir for the fluid coming from the PWM valve. The higher the amount of fluid in the intermediate chamber the higher the average intermediate pressure value will be. The transient behavior of the valve was estimated by providing a squared PWM signal as input data to the mathematical model. The time during which the valve remains opened or closed is determined by the duty cycle, which also sets the valve flow coefficient either to the nominal value or to zero.

5. RESULTS

5.1 Adiabatic capillary tubes

5.1.1 Experimental results

The 24 data points of the test matrix cover a range of mass flow rates between 0.29 kg/h and 2.93 kg/h, typical of meso-scale cooling systems. The extra 20 data points widen this range, covering flow rates up to 3.95 kg/h. The main and confounding effects are shown in Figure 2. It is worth noting that, as expected, the capillary tube I.D. plays a major role in determining the refrigerant mass flow rate. It can also be seen that the effects of both the capillary tube length and condensing pressure are similar but opposite to each other. Of the four factors addressed in this study, the subcooling had the most discreet effect.

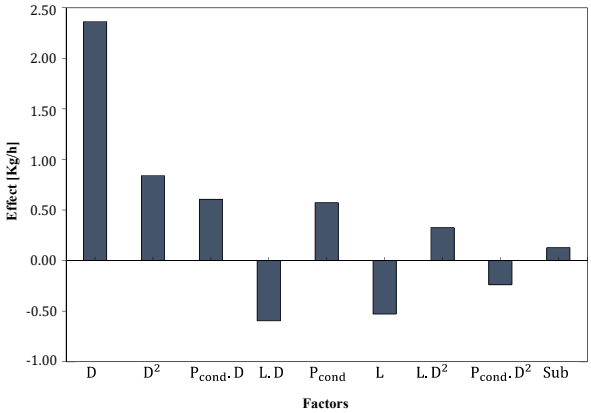

Figure 2: Main and confounding effects of adiabatic capillary tubes

The non-linear behavior of the confounding effects of the diameter, D^2, condensing pressure-diameter, $P_{cond}.D^2$, and length-diameter, $L.D^2$, merit some attention. These three parameters highlight the great importance of the inner diameter on the capillary tube flow in meso-scale cooling applications. The confounding effect of the inner diameter D^2, for instance, can be understood as an extra contribution to the main effect of the diameter.

5.1.2 Empirical correlation

An empirical correlation was fitted to the factorial experimental database of 24 data points, through the least squares method. The correlation coefficients are shown in Table 3.

$$\dot{m} = C1 + C2 \cdot D + C3 \cdot D^2 + C4 \cdot P_{cond} \cdot D + C5 \cdot L \cdot D + C6 \cdot P_{cond} + C7 \cdot L + \\ + C8 \cdot L \cdot D^2 + C9 \cdot P_{cond} \cdot D^2 + C10 \cdot Sub + C11 \cdot Sub \cdot D \quad (1)$$

Figure 3 shows the relative errors between the predictions obtained with equation (1) and the 44 experimental data points. It can be observed that the deviations are lower than ± 10% for all points of the factorial database. It can also

be seen that the correlation predictions are reasonably good for diameters ranging from 0.23mm to 0.45mm, with only two points lying outside the ± 10% band. On the other hand, it is clear that the proposed correlation does not capture the physics behind larger diameter capillary tubes (e.g., 0.53mm).

Table 3: Empirical coefficients – adiabatic capillary tube

C1	C2	C3	C4	C5	C6	C7	C8	C9	C10	C11
2.867	0.086	-0.001	-18.024	32.494	-0.042	-0.648	1.439	0.009	-0.017	0.193

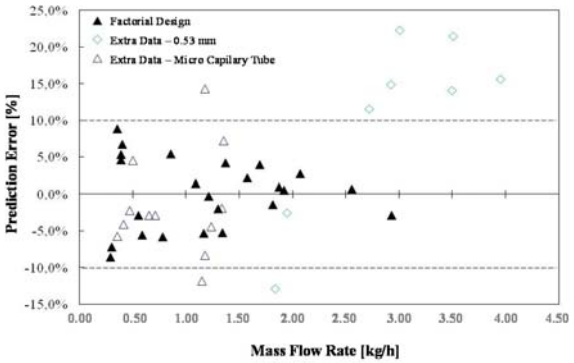

Figure 3: Correlation predictions vs. experimental data

5.1.3 Differential model

Figure 4a compares the predictions of the differential model with the experimental data. The results highlight, once again, the effect of the inner diameter on the discrepancy level. It was observed that the deviations remain within a ± 10% error band for regular I.D. (0.531mm) capillary tubes. The lower the I.D. the higher the discrepancy. The adopted correlations for the refrigerant viscosity and friction factor are probably not applicable to smaller I.D. capillary tubes. A correction for the friction factor was thus proposed, as follows,

$$f = f_C \cdot 1.13 - e^{-3000.D} \quad (2)$$

where f_c is the Churchill friction factor and D the inner diameter of the capillary tube.

The differential model predictions, this time with the proposed friction factor correction factor, are shown in Figure 4b. It is worth noting that all deviations related to the smaller I.D. capillary tubes remained within an error band of ± 10%. Comparisons were also carried out with the database gathered by Boabaid et al. (1994), for regular I.D. capillary tubes (0.606mm to 1.05mm). It can be seen that the model predictions are also good for this diameter range, with most of the deviations (91%) lying within a ±10% error band.

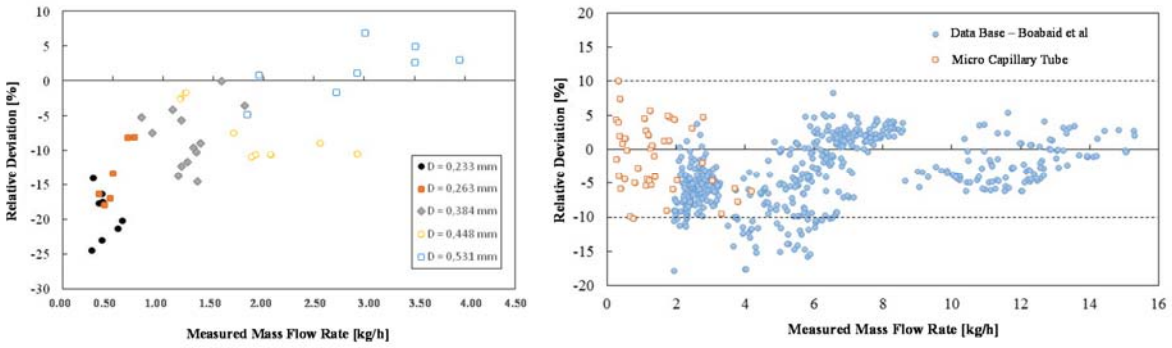

(a) (b)

Figure 4: Relative error vs. mass flow rate: differential model (a) without and (b) with correction factor

5.1.4 Algebraic model

Figure 5a compares the algebraic model predictions with the experimental data. It can be noted that the algebraic model also tends to underestimate the mass flow rates through small diameter capillary tubes, with only 65% of the predictions lying inside a ± 10% error band. Since the ∅ = 6 factor derived by Hermes et al. (2010) is directly related to the friction factor, a similar correction factor was also proposed for this parameter, as follows,

$$\emptyset = -3.45.D^{-0.0081} \quad (3)$$

With this correction factor in place, the algebraic model predicted 100% of the small diameter and 91% of the regular diameter capillary tube mass flow rates within a ± 10% error band, as illustrated in Figure 5b.

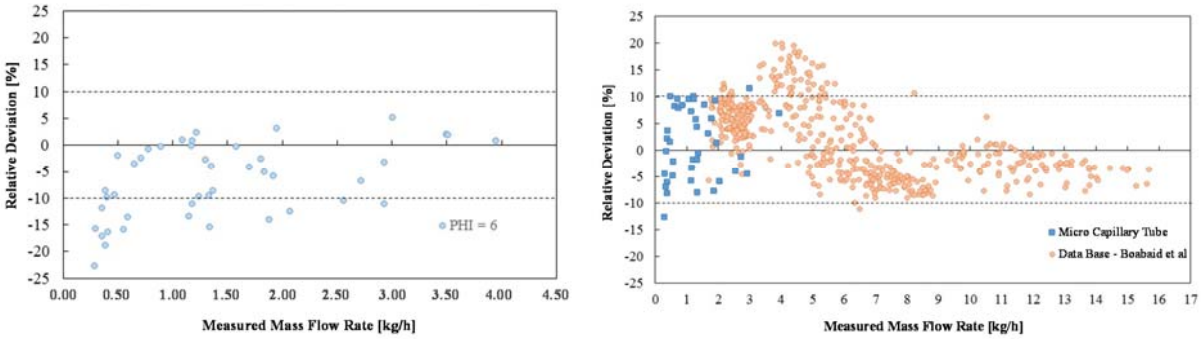

(a) (b)

Figure 5: Relative error vs. mass flow rate: algebraic model (a) without and (b) with correction factor

5.1.5 Visualization

In order to study the effect of vapor bubbles entering the small-sized capillary tubes, experiments were carried out with a high-speed camera to visually monitor the refrigerant flow through a 0.45mm I.D., 1 m length capillary tube, subject to an inlet pressure of 19bar. The experiment started with a subcooling of 5ºC and a mass flow rate of 2.6 kg/h. The subcooling was then progressively reduced and thus the refrigerant mass flow rate also decreased. As shown in Figure 6a, mist and flow disturbances start to appear when the subcooling reaches values of the order of 2ºC. At 1ºC, small bubbles and oscillations in the refrigerant mass flow rate are clearly noted. Small bubbles start to appear when the quality reaches 0.7%, most of which implode before reaching the capillary, as shown in Figure 6b.

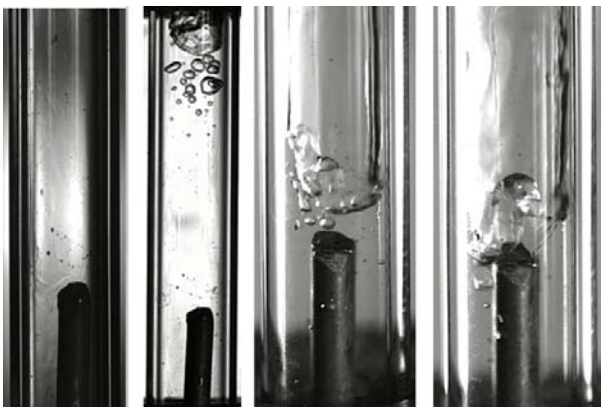

(a) (b) (c) (d)

Figure 6: Flow pattern at the entrance of the capillary tube (a) inlet quality=0%, (b) 0.7%, (c) 1.3% and (d) 2.0%

At around an inlet quality of 1.3%, a liquid membrane starts to appear close to the border of the capillary tube, being periodically broken by vapor slugs and swirls, as shown in Figure 6c. At this stage, the mass flow rate drops by approximately 30%. Finally, Figure 6d shows that the flow tends toward an annular pattern when the quality reaches

values of the order of 2.0%. At this stage, only vapor passes through the sight glass and the mass flow rate drops to 1.2 kg/h, a value 50% less than that observed when only liquid is present at the entrance of the capillary tube.

The results of these experiments show that the mass flow rate drops almost linearly with a drop in the subcooling. It was also observed that small bubbles at the entrance of the capillary tube cause a deviation from the linear decay as well as from the numerical model predictions. It is thus evident that the vapor bubbles at the entrance of capillary tubes are more critical at the meso-scale compared with regular-sized cooling systems.

5.2 Pulsating capillary tubes

5.2.1 Experimental results

These experiments considered mass flow rates ranging from 0.48 kg/h to 3.15 kg/h. The effects of each variable and their interactions with the mass flow are shown in Figure 7. Of the main effects, the duty cycle (DC) appears to be the most significant factor. The intermediate chamber internal volume, V, and the flow coefficient, K, have similar and irrelevant effects, while the pulse period, τ, has a negligible effect of the order of the experimental uncertainties.

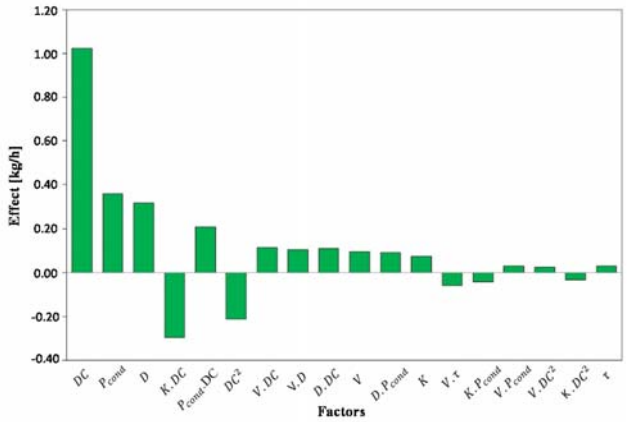

Figure 7: Main and confounding effects of pulsating capillary tubes

The most significant confounding effects are the flow coefficient-duty cycle, K.DC, the condensing pressure-duty cycle, P_{cond}.DC, and the non-linear effect of the duty-cycle, DC^2. The K.DC confounding effect means that the larger the valve orifice the lower the effect of the duty cycle on the mass flow rate. The P_{cond}.DC effect has a similar but opposite meaning. The duty cycle quadratic effect means that the lower the duty cycle the higher the effect on the mass flow rate.

5.2.2 Empirical correlation

The experimental data were used to derive an empirical correlation for the mass flow rate. To this end, only the variables with the most significant effects on the mass flow rate were taken into account, as shown in equation (4). The coefficients are given in Table 4.

$$\dot{m} = j1 + j2 \cdot K + j3 \cdot V + j4 \cdot D + j5 \cdot P_{cond} + j6 \cdot D + j7 \cdot DC^2 + j8 \cdot K \cdot DC + \\ + j9 \cdot V \cdot D + j10 \cdot V \cdot DC + j11 \cdot D \cdot P_{cond} + j12 \cdot D \cdot DC + j13 \cdot P_{cond} \cdot DC \quad (4)$$

Table 4: Empirical coefficients – pulsating capillary tube

j1	j2	j3	j4	j5	j6	j7
4.0957E+00	1.1166E+07	-1.6718E-01	-8.9665E+00	-2.2049E-01	-4.0783E-04	-1.3354E-04
j8	**j9**	**j10**	**j11**	**j12**	**j13**	**j14**
-1.8545E+05	3.3905E-01	2.8945E-04	4.9424E-01	4.5174E-02	8.5892E-04	-

Figure 8 compares the predictions of equation (4) with the experimental data, extended with some data gathered with a third intermediate flow coefficient valve. Unfortunately, the correlation does not reproduce the experimental data as expected, with deviations of the order of ± 30%.

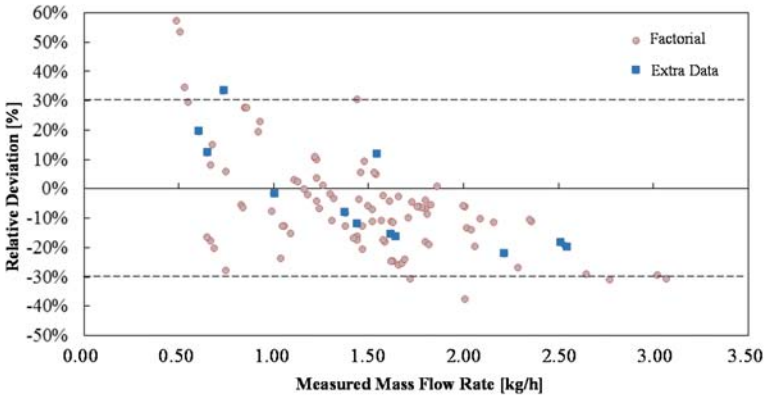

Figure 8: Relative error vs. mass flow rate – empirical equation

5.2.3 Numerical model

Figure 9 compares the predictions of the model described by Ronzoni et al. (2011) with the entire set of experimental data, including those obtained by the author for regular-sized capillary tubes. It can be noted that the model predictions are reasonably close (± 10%) to the experimental data for regular-sized capillary tubes. In contrast, deviations of the order of ± 30% are observed for smaller capillary tubes. Unfortunately, the tuning of the model described by Ronzoni et al. for the entire range of capillary tubes is not a straightforward task, due to the complexity of the phenomena involved.

5.2.4 Visualization

A glass intermediate chamber was constructed and used to visually monitor the refrigerant flow. All of the experiments were carried out with a condensing temperature of 35°C, a 0.448mm I. D. capillary tube and a 7.96E-8 flow coefficient valve. Figure 10a shows the results obtained with a 1ml intermediate volume, a 1s pulse period and a 10% duty cycle. It is worth noting that during part of the period the liquid level remains close to the border of the capillary tube while in another part it lies below this border. The liquid level is restored with the opening of the valve. Under these conditions, the average mass flow rate reaches values of the order of 0.9kg/h. Figure 10b shows the flow regime under the same operating conditions, but with a duty cycle of 50%. Under these conditions the refrigerant mass flow rate attains values of the order of 1.2 kg/h, and a permanent oscillating liquid membrane is clearly seen in the middle of the chamber. Figure 10c was obtained with a duty cycle of 90%, showing that under these conditions the chamber is almost entirely filled with liquid. From these pictures it can be concluded that the refrigerant mass flow rate is strongly affected by the duty cycle, corroborating the previous experimental results.

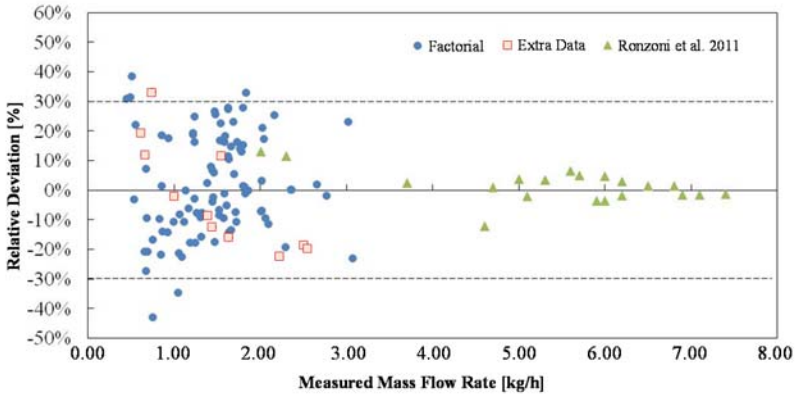

Figure 9: Relative error vs. mass flow rate – numerical model

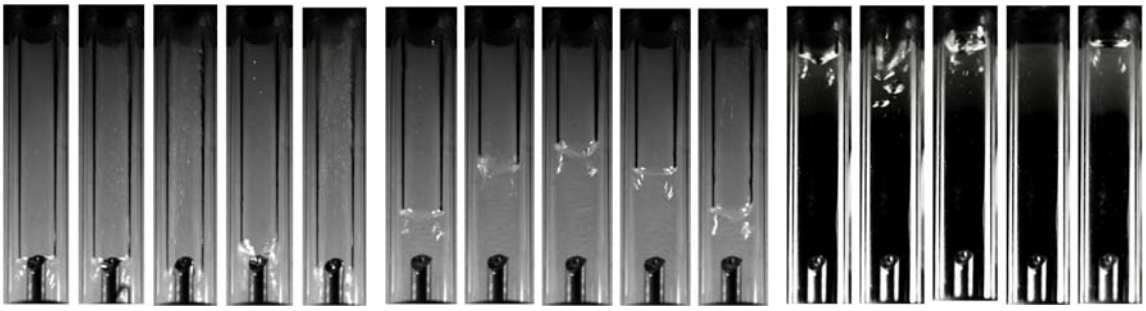

(a) (b) (c)

Figure 10: Intermediate chamber flow regimes: (a) DC=10%, (b) DC=50% and (c) DC=90%

6. CONCLUDING REMARKS

The aim of this study was to investigate the HFC-134a flow through fixed and variable restriction expansion devices, specifically for meso-scale cooling systems. Thirty-six experiments were carried out with adiabatic capillary tubes, with mass flow rates ranging from 0.29kg/h to 3.95 kg/h. The results show that the internal diameter has the greatest effect on the mass flow rate, followed by its non-linear effect. The derived empirical equation predicted most of the experimental data within an error band of ±10%, with only two data points lying outside this band. The visualization studies showed that the capillary tube flow is strongly affected by vapor bubbles at the entrance of the capillary tube, which has a strong impact on the refrigerant mass flow rate. An algebraic and a differential model were both used to predict the refrigerant flow through capillary tubes. With the use of a model the mathematical predictions tended to underestimate the experimental values and correction factors were therefore proposed for both models, which afforded performance improvements.

Ninety-six experiments were also carried out with pulsating capillary tubes, with mass flow rates ranging from 0.48kg/h to 3.15kg/h. It was shown that the valve duty cycle determines the mass flow rate, and that the pulse period and flow coefficient play an insignificant role. Both the empirical and numerical model were not able to properly predict the refrigerant mass flow rate, with deviations of the order of ± 30%. The visualization studies offered a better understanding of the dynamics of the refrigerant flow through pulsating capillary tubes.

REFERENCES

Bittle R. R., Weis S. R., 2002, New insights into two-phase viscosity models used in capillary tube flow models. Private communication.

Boabaid Neto, C. B., 1994, Análise do desempenho de tubos capilares adiabáticos, Master's Thesis, Federal University of Santa Catarina, Florianópolis, SC, Brazil.

Bolstad, M. M., Jordan, R. C., 1948, Theory and Use of the Capillary Tube Expansion Device. Journal of the ASRE - Refrigerating Engineering (December), 519-523.

Box, G. E. P., Hunter, W. G., Hunter, J. S., 1978, Statistics for experimenters. An introduction to design, data analysis, and model building, John Wiley & Sons, New York, NY, USA.

Carnahan, B., Luther, H. A., Wilkes, J. O., 1969, Applied numerical methods, John Wiley & Sons, New York, USA.

Churchill S. W., 1977, Friction factor equation spans all fluid flow regimes, 12th International Congress of Refrigeration, Madrid, Spain, pp. 1069-1077.

Gonçalves, J. M., 1994, Análise experimental do escoamento de fluidos refrigerantes em tubos capilares, Dissertação de Mestrado, Universidade Federal de Santa Catarina, Florianópolis, SC, Brasil.

Hermes, C. J. L., 2006, Uma metodologia para a simulação transiente de refrigeradores domésticos, PhD Thesys, Federal University of Santa Catarina, Florianópolis, SC, Brazil, p.273.

Hermes, C. J. L., Melo, C., Knabben, F. T., 2010, Algebraic solution of capillary tube flows. Part I: Adiabatic capillary tubes", Applied Thermal Engineering, Vol. 30, pp. 449-457.

IIR, T., Council, T. A., 2010, Word from the Director IIR listing of refrigeration research priorities. International Journal of Refrigeration, v. 28, n. 7, p. 973-976.

Jeong, S. A., 2004, quel point estil difficile de réaliser un réfrigérateur miniaturisé? International Journal of Refrigeration, v. 27, n. 3, p. 309-313.

Marcinichen, J. B., Melo, C., 2006, Comparative analysis between a capillary tube and an electronic expansion valve in a household refrigerator. Refrigeration and air conditioning, p. 1-8.

Melo, C., Ferreira, R.T.S., Pereira, R. H., 1992, Modeling Adiabatic Capillary Tubes: A Critical Analysis. Proc. of the International Refrigeration and Air Conditioning Conference at Purdue. pp. 113-122.

Melo, C., 1999, An experimental analysis of adiabatic capillary tubes. Applied Thermal Engineering, v. 19, n. 6, p. 669-684.

Mikol, E. P., Dudley, J. C., 1964, A visual and photographic study of the inception of vaporization in adiabatic flow, Journal of Basic Engineering, [S. 1.], pp. 257-264.

Pottker, G., Melo, C., 2007, Experimental study of the combined effect of the refrigerant charge, compressor speed and expansion valve opening in a refrigeration system. P. 1-8.

Ronzoni, A. F., Hermes, C. J. L., Melo, C., 2011, A study of PWM-induced flows through serial expansion valve / capillary tube arrangements. Graduation Degree. Federal University of Santa Catarina, Florianópolis, SC, Brazil.

Thiessen, M.R., Klein, F.H, 2007, Flow rate control system in refrigeration circuits, method for controlling a refrigeration system, World Intellectual Property Organization, Patent WO 2007/118293 A2.

Zhang, C., Ma, S., Chen, J., Chen, Z., 2006, Experimental analysis of R22 and R407c flow through electronic expansion valve. Energy Conversion and Management, v. 47, n. 5, p. 529-544.

ACKNOWLEDGEMENTS

This study was made possible through the financial funding from the EMBRAPII Program (POLO/UFSC EMBRAPII Unit - Emerging Technologies in Cooling and Thermophysics). The authors thank Embraco S.A. for financial and technical support.